Aqueous U(VI) removal by green rust and vivianite at phosphate-rich environment

Youngho Sihn[*] and In-Ho Yoon[a]

Decommissioning Technology Research Division, KAERI, Daejeon 34057, Korea

Abstract. Vivianite ($Fe_3^{2+}(PO_4)2 \cdot 8H_2O$) and green rust ($[Fe_4^{2+}Fe_2^{3+}(OH)^-_{12}][SO_4^{2-} \cdot 2H_2O]^{2-}$), ferrous containing minerals, could remove aqueous U(VI) in 5 min. and the efficiencies of green rust were roughly 2 times higher than that of vivianite. The zeta potential measurement results implies that the better performance of green rust might be attributed to the favorable surface charge toward uranyl phosphate species. The removal behaviors of the minerals were well fitted by pseudo-second order kinetic model ($R^2 > 0.990$) indicating the dominant removal process was chemical adsorption. Effects of Ca^{2+} and CO_3^{2-} at pH 7 were examined in terms of removal kinetic and capacity. The kinetic constants of aqueous U(VI) were 8 and 13 times lower (0.492×10^{-3} g/(mg·min); 0.305×10^{-3} g/(mg·min)) compared to the value in the absence of the ions. The thermodynamic equilibrium calculation showed that the stable uranyl species (uranyl tri-carbonate) were newly formed at the condition. Surface investigation on the reacted mineral with uranyl phosphates species were carried out by XPS. Ferrous iron and U(VI) on the green rust surface were completely oxidized and reduced into Fe(III) and U(IV) after 7 d. It suggests that the ferrous minerals can retard U(VI) migration in phosphate-rich groundwater through the adsorption and subsequent reduction processes.

Keywords: uranium; vivianite; green rust; phosphate complexes; adsorption; remediation

1. Introduction

Power plant and weapon industries in many countries have extensively used a uranium (U) as a raw material. It requires a large quantity of U supply that involving U handling process such as mining, milling, and purification. An enormous volume of U waste were generated from the process and its accidental leakage causes radioactive contamination of subsurface environment (Amaral *et al.* 1998, Alves *et al.* 2004, Peterson *et al.* 2008). Released U migrates along the groundwater pathways as hexavalent form (U(VI)) and its mobility is determined by the interaction with natural materials including clay, metal-oxides, and microbes, etc (Gavrilescu *et al.* 2009, Selvakumar *et al.* 2018).

Sorption is one of the dominant interaction at water-mineral interfaces that retards U(VI) migration in the groundwater. Ferrous minerals are abundant natural materials and numerous studies have reported that the mineral could adsorb the aqueous U(VI) on its surface. Magnetite (Fe_3O_4), mixed ferrous/ferric mineral formed by abiotic corrosion or microbial transformation, showed effective removal of aqueous U(VI) from MQ water at circumneutral pHs (Missana *et al.* 2003, Aamrani *et al.* 2007, Das *et al.* 2010, Crane *et al.* 2011). It could uptake more than 20% of aqueous U(VI) even from environmental water (Crane *et al.* 2011).

Mackinawite (FeS) is a ferrous sulfide mineral and it completely separated aqueous U(VI) in several hours via $Fe^{2+}_{surface}$ exchange at wide range of pHs (Livens *et al.* 2004, Hua and Deng 2008, Hyun *et al.* 2012, Gallegos *et al.* 2013). Pyrite (FeS_2) also adsorbed aqueous U(VI) on its $\equiv$Fe-OH and $\equiv$S-SH sites coupled with deprotonation process (Eglizaud *et al.* 2006, Scott *et al.* 2007, Descostes *et al.* 2010). The ferrous minerals not only adsorb U(VI) but also subsequently and/or simultaneously reduced it into immobile U(IV) by donating electrons from the surface ferrous/sulphide phases, thereby, the ferrous minerals have attracted a great attention as an in-situ remediation approach for long-term retardation of U(VI) transport.

Green rust ($(Fe_4^{2+}Fe_2^{3+}(OH^-)_{12})^{2+}(Anion \cdot 2H_2O)^{2-}$) and vivianite ($Fe_3^{2+}(PO_4)_2 \cdot 8H_2O$) are the secondary ferrous minerals that typically found in iron reducing environments. Green rust is the product of reduction of hydrous ferric oxides/oxyhydroxides by a metal-reducing bacterium. In phosphate-rich condition, vivianite is an end-product of the microbial ferric reduction. The biogenic minerals have been reported that effectively de-chlorinate and adsorb a wide range of environmental contaminants including chlorinated compounds, As(V), Cr(VI), Se(VI), Cu(II), Hg(II), etc (Bond and Fendorf 2003, O'Loughlin *et al.* 2003, Hudson-Edwards *et al.* 2008, Jonsson and Sherman 2008, Bae and Lee 2012, Schellenger and Larese-Casanova 2013). Previous XAFS studies confirmed that the adsorbed U(VI) on the green rust and vivianite surface was reduced into nano crystalline uraninite (UO_2) and monomeric U(IV) particles, respectively (O'Loughlin *et al.* 2003, O'Loughlin *et al.* 2010, Veeramani *et al.* 2011). It suggests that green rust and vivianite can play an effective barrier role in the

---

*Corresponding author, Ph.D.
E-mail: sihnyh@kaeri.re.kr
[a] Ph. D.

subsurface transport of aqueous U(VI). In addition, geochemical factors in the subsurface affect interaction of aqueous U(VI) with mineral surface. Phosphate and carbonate, major ions in groundwater, have been known that those can enhance or hinder the U(VI) adsorption performance of the iron minerals (Payne *et al.* 1996, Romero-Gonzalez *et al.* 2007, Cheng *et al.* 2007, Bachmaf *et al.* 2008, Singh *et al.* 2012).

In this study, the surface reaction of aqueous U(VI) with sulfate-green rust (GR) and vivianite (Viv) were investigated in the phosphate-rich conditions. Adsorption kinetics of U(VI) on the minerals were determined considering effects of solution pHs and major groundwater ions such as calcium (Ca^{2+}) and carbonate (CO_3^{2-}). The chemical species on the mineral surface were examined by X-ray spectroscopy to identify the surface reaction process.

2. Materials and methods

2.1 Materials

All chemicals in the experiments were ACS grade or higher and used without further purification. For the mineral synthesis, ammonium ferrous sulfate hexahydrate [$(NH_4)_2Fe(SO_4)_2·6H_2O$, 99.997%, Sigma-Aldrich], anhydrous sodium acetate (CH_3COONa, >99%, Aldrich), sodium phosphate dibasic (Na_2HPO_4, 99.95%, Aldrich), sodium hydroxide (NaOH, >97%, Aldrich) were used. Phosphate buffer system were prepared with potassium phosphate monobasic (KH_2PO_4, > 99%, Aldrich) and Na_2HPO_4. Calcium hydroxide ($Ca(OH)_2$, >95%, Aldrich) and sodium bicarbonate ($NaHCO_3$, >99.7%, Aldrich) were used in the experiments of groundwater ions effect. Uranyl nitrate hexahydrate ($UO_2(NO_3)_2·6H_2O$, 98 – 102%, Fluka) was dissolved in $1x10^{-1}$ M $HClO_4$ to prepare $1X10^{-3}$ M U(VI) stock solution. All the experiments were conducted in an anaerobic chamber (atmospheric condition: 95% $N_{2(g)}$ and 5% $H_{2(g)}$, Coy Laboratory Products Inc.) and the solutions were made using deaerated deionized water (DDW, resistivity > 18.2 MΩcm) purged by $N_{2(g)}$ for 24 h. GR and Viv were synthesized according to the previously our reported method (Sihn *et al.* 2013, Bae *et al.* 2018). Briefly, aqueous Fe(II) was mixed with phosphate solution to obtain Viv precipitates. GR was synthesized by precipitating Fe(II)/Fe(III) solution at alkaline condition.

2.2 Materials

Batch adsorption experiments were carried out in duplicate with 24 mL polytetrafluoroethylene (PTFE) vial at 25±°C and each sample representing one data point. An aliquot amount of the minerals (GR and Viv) was transferred into the vial containing 23 mL of 0.2 M phosphate buffer (mixture of 9.36 g/L KH_2PO_4 with 32.73 g/L Na_2HPO_4) solution adjusted at pH 7. Initial Fe(II) concentration in the suspension was 1 mM and an exact amount of U(VI) stock solution was injected into the vial, i.e., [U(VI)]$_{initial}$ = 1 μM, to initiate the reaction. Vials were immediately capped and transferred into the gastight container filled with N_2 gas. It was mounted on the end-over-

end rotator at 0.5 rpm and the sample was periodically sacrificed to quantify aqueous U concentration. The suspension was filtered through 0.2 μm nylon filter and the filtrate was 10 times diluted with 4% HNO_3 solution to determine aqueous U concentration by Inductively Coupled Plasma-Mass Spectrometry (ICP-MS, Perkin-Elmer, Elan 6000). In the experiments of pH effect, suspension pH was pre-adjusted to 5 and 9 by adding a few drops of 1 M $HClO_4$ and NaOH solution. Calcium hydroxide and sodium bicarbonate were used to determine the groundwater ion effects on the U(VI) interaction with the GR and Viv.

2.3 Analysis

The synthesized mineral phases were identified by high-resolution powder X-ray diffractometer (Rigaku, Smartlab) with Cu Kα radiation. The dried sample was scanned at 2θ from 10° to 70° range at a scan rate of 2°·min^{-1}. Surface area of the minerals were measured by Brunauer-Emmett-Teller (BET) method using Micromeritics, 3 Flex. Prior to the measurement, the sample was degassed at 150°C for 2 h. The surface charge of the minerals were determined by zeta-potential analyzer (ELS-Z2, Otsukael). The mineral suspension in 0.1 M $HClO_4$ was manually shaken for 2 min. and let the aggregated particles settle for 5 minutes through gravitational settling. The supernatant was taken and titrated to the target pH by adding 1 M $HClO_4$ and NaOH. X-ray photoelectron Spectroscopy (XPS, Thermo Scientific, K-alpha) analysis have investigated the redox states of U **$4f_{7/2}$** and Fe **$2p_{3/2}$** on the reacted mineral surfaces. The reacted mineral suspension was vacuum filtered through 0.2 μm nylon filter and the collected solid phase was washed with DDW for 3 times. The sample was freeze-dried for 2 d. It was suspended in the N_2-purged ethanol and immediately transferred to the XPS vacuum chamber to prevent oxygen contact from air. XPS analysis was conducted with 20 eV of pass energy; 50 msec of dwell time; 15 times narrow scan. The charge shift effect was corrected using the C 1s peak at 284.8 eV as a standard value.

3. Results and discussions
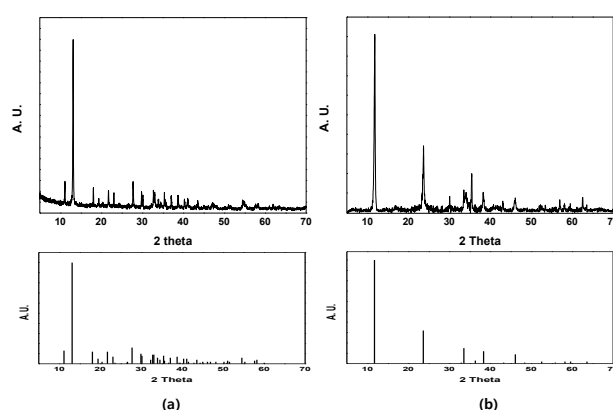
3.1 Aqueous U(VI) removal by the minerals

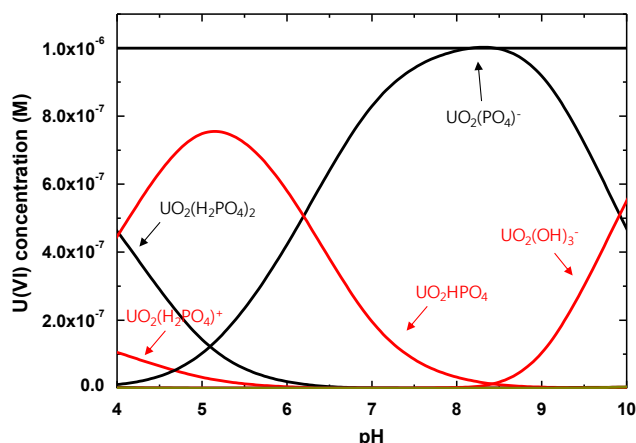Fig. 1 XRD pattern of the synthesized (a) Vivianite (b) Sulfate-Green rust

Fig. 2 Chemical distribution of aqueous U(VI) species in the phosphate buffer solution

Fig. 3 (a) Aqueous U(VI)-phosphates removal and (b) its kinetic (pseudo-second-order fitting) in GR and Viv suspension at pH 7

The purity of the synthesized GR and Viv were confirmed by XRD analysis as shown in Figure 1. The measured peak positions and relative intensities were consistent with the reference data (ICDD database) confirming successful synthesis of the minerals. The U(VI) stock was diluted in the 0.2 M phosphate buffer solution at pH 7. Figure 2 showed the chemical species of aqueous U(VI) that calculated by thermodynamic equilibrium modelling program (Visual Minteq 3.1). The uranyl phosphate species, UO_2HPO_4 and $UO_2(PO_4)^-$, are found to be dominant at pH 7 and it agrees well with the experimental results in our previous laser spectroscopy study (Sihn *et al.* 2016).

Aqueous U(VI) was rapidly removed by GR and Viv at pH 7 (Figure 3). The control sample showed the constant U(VI) value indicating aqueous U(VI) did not interact with inner-surface of the vial. In the presence of the minerals, aqueous U(VI) concentration was rapidly reduced and it reached equilibrium-state plateau after 5 min. GR removed more than 97% of U(VI) in 5 min. while 62% of U(VI) was removed by Viv. It was slowly increased up to 70% after 24 h. The removal kinetics by the minerals were fitted with pseudo-second order kinetic model as follows.

$$\frac{t}{q_t} = \frac{1}{kq_e^2} + \frac{t}{q_e} \tag{1}$$

where q_t [mg·g^{-1}] and q_e [mg·g^{-1}] are the amounts of adsorbed U(VI) at specific and equilibrium times, respectively; t is reaction time [min]; k is pseudo-second order rate constant [g·(mg·min)$^{-1}$].

The model was found to show the best fit for the removal behaviour as shown in Figure 1(b) ($R^2 > 0.999$). This good agreement indicates that the U(VI) removal by the minerals were occurred via the chemisorption process (Ho and Mckay *et al.* (1999)). The calculated rate constants were 5.05×10^{-2} g·(mg·min)$^{-1}$ for GR and 3.91×10^{-3} g·(mg·min)$^{-1}$ for Viv. The estimated adsorption capacity of GR (53.48 mg·g^{-1}) were also higher compared to that of Viv (32.62 mg·g^{-1}). The results demonstrated that the GR could remove aqueous U(VI) with 1.6 times higher quantity and 13 times faster kinetic than Viv.

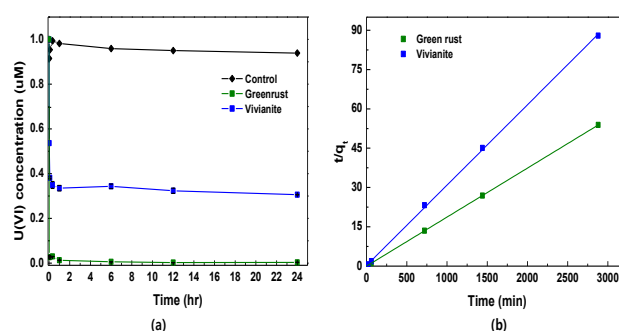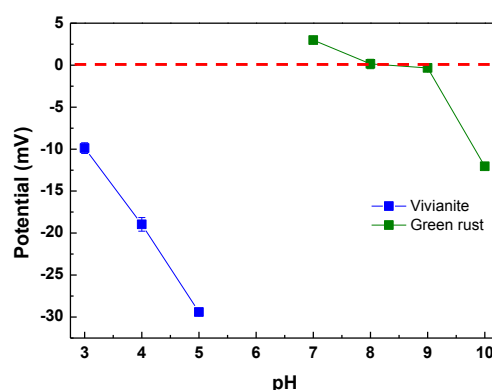Fig. 4 Zeta potential curve as a function of pH for GR and Viv

Zeta potential of the minerals were measured as a functional of suspension pH (Figure 4). At pH 3, the surface charge of Viv was -9.9 mV and the tendency was increased as pH increases (-29.4 mV at pH 5). GR surface showed positively charged value (+3.0 mV) at pH 7 and it was shifted to the negatively charged region (-0.3 mV) at pH 9. At the reaction pH (pH 7), the results revealed that Viv surface was negatively charged while GR surface was weak positively charged. The initial U(VI) species were 80% of $UO_2(PO_4)^-$ with 20% UO_2HPO_4 (Figure S2), therefore, the electrostatic attractive force between U(VI) species and GR surface might result in the rapid and complete adsorption of U(VI). The limited U(VI) adsorption by Viv could be attributed to the electrostatic repulsive force between negatively charged surface and U(VI) species. It indicates that the removal of U(VI)-phosphate complexes by the minerals would be dependent on the charge-charge interaction at water-mineral interfaces.

3.2 pH and anion/cation effects

The effect of solution pH and major ions were investigated by means of batch experiments. Aqueous U(VI) concentration in reacting with the minerals were monitored from acidic to alkaline pH conditions (Figure 5
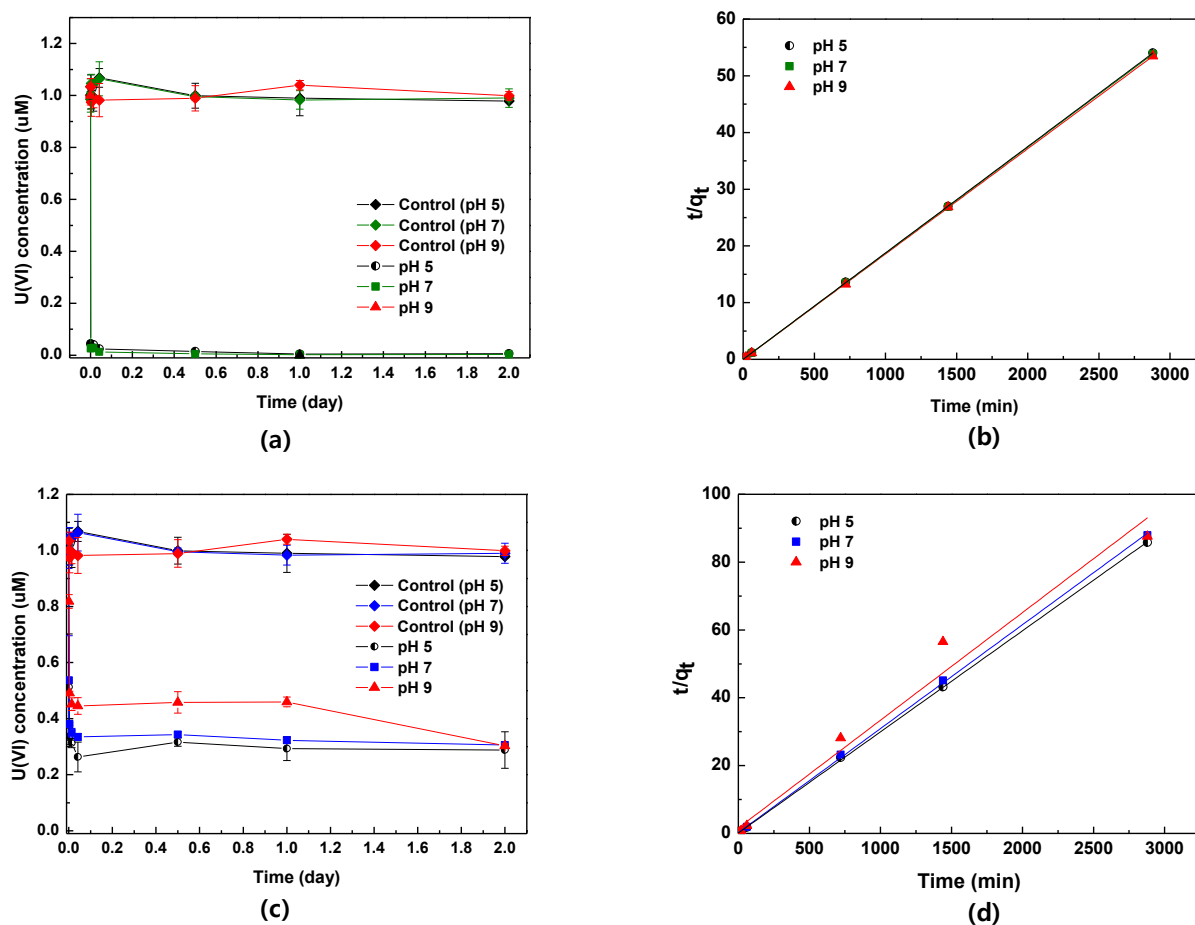
Fig. 5 Aqueous U(VI)-phosphates removal by (a) GR and (c) Viv and its kinetic (pseudo-second-order fitting) of (b) GR and (d) Viv at different pH conditions

(a) and (c)). GR could remove more than 95% of aqueous U(VI) in 1 min. at all the suspension pHs. Viv quickly removed aqueous U(VI) in 5 min. and the efficiencies were decreased as pH increases ($\eta_{removal}$ = 66% at pH 5; $\eta_{removal}$ = 62% at pH 7; $\eta_{removal}$ = 51% at pH 9). After 5 min., aqueous U(VI) concentration was slowly reduced and the final efficiencies were 69-71%. The results showed that GR can completely adsorb U(VI)-phosphate complexes at the groundwater pHs. However, Viv performance would be limited at basic conditions. Figure 5 (b) and (d) demonstrate the kinetic fitting results at different pHs. The model ($R^2 >$ 0.979 – 0.999) nicely fit the adsorption behavior. The kinetic constants of GR were 2.15 – 5.05 x 10^{-2} g·(mg·min)$^{-1}$ at pH 5 – 9 and 7 – 80 times lower kinetic constants were obtained by Viv as 7.39 – 0.63 x 10^{-3} g·(mg·min)$^{-1}$ at pH 5 – 9. The calculated adsorption capacities of GR (53.3 – 53.9 mg·g^{-1}) were higher than that of Viv (31.5 – 33.5 mg·g^{-1}) in a range of pH 5 to 9.

The chemical distribution of U(VI) complexes were predicted as a function of pH (Figure 2). The uranyl phosphates (UO$_2$HPO$_4$/UO$_2$(H$_2$PO$_4$)$_2$) were dominant at pH 5, however, the species were converted to UO$_2$(PO$_4$)$^-$/UO$_2$(OH)$_3$$^-$ at pH 9. The surface charge of the minerals

were measured (Figure 4) and the zero charge value of GR was 8.35. Viv showed much lower value as 3.3. The results indicate GR surface was positively charged at acidic to weakly basic condition, therefore, it facilitates adsorbing neutrally/negatively charged U(VI) species. However, negatively charged Viv surface over pH 3 was not feasible to adsorb neutral/negatively charged U(VI). In conclusion, U(VI) adsorption performance of the minerals would be determined by its surface charge properties toward uranyl species at groundwater conditions.

As shown in Figure 6(a) and (c), the effects of Ca^{2+} and HCO$_3$$^-$ were investigated on the U(VI) adsorption by the minerals. The typical value of the ions in groundwater, Daejeon; South Korea, were used as [Ca^{2+}]=15 ppm and [HCO$_3$$^-$]=80 ppm. In GR suspension, aqueous U(VI) over 95% was removed in 1 min. and it did not desorb for 48 h. It proved that the U(VI) adsorption performance of GR was maintained in the presence of Ca^{2+} and HCO$_3$$^-$. Viv could remove 62% of aqueous U(VI) in 5 min. and the efficiencies were reduced by adding Ca^{2+} ($\eta_{removal}$ = 44%) and HCO$_3$$^-$ ($\eta_{removal}$ = 29%). The values were slowly increased to 69-73% after 48 h. The experimental data were fitted by the pseudo-second order kinetic model (Figure 6
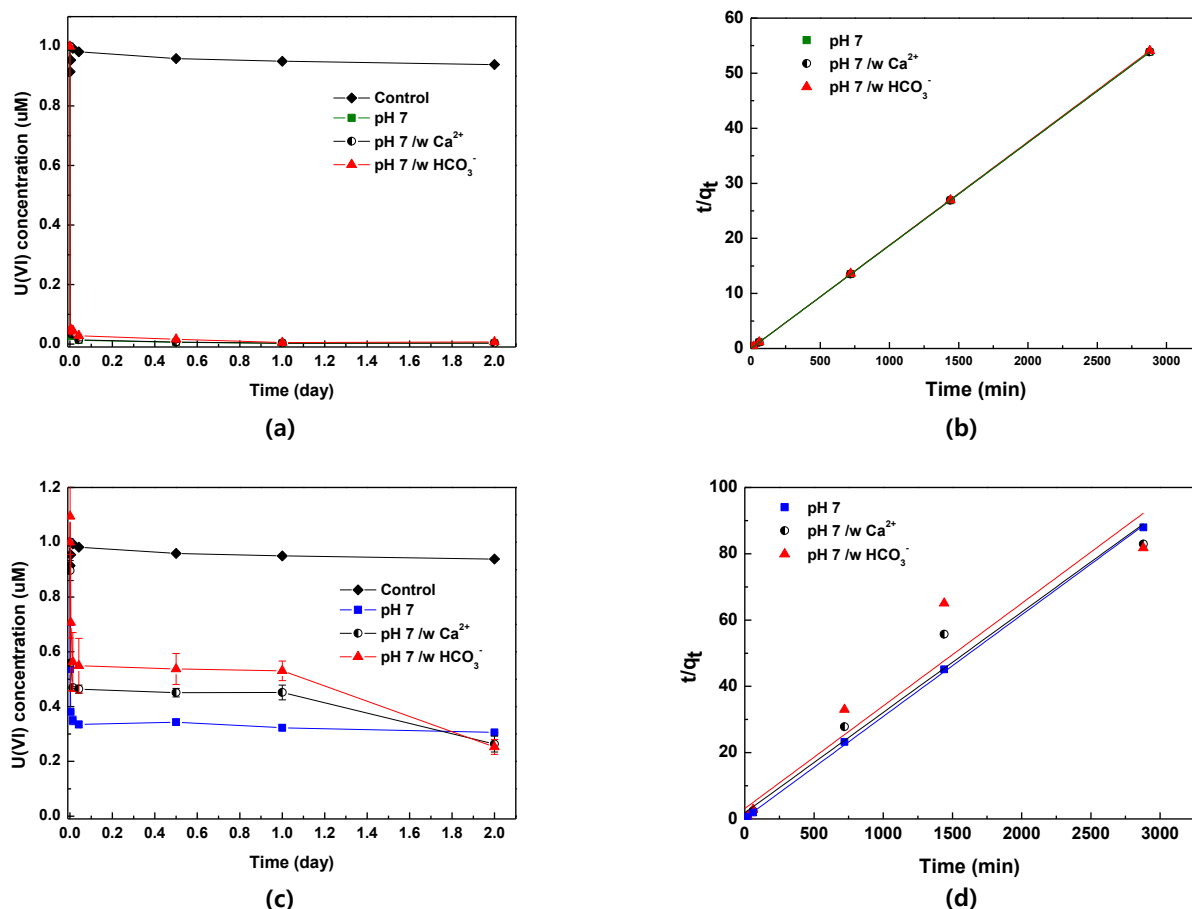
(a)

(b)

(c)

(d)

Fig. 6 Aqueous U(VI)-phosphates removal by (a) GR and (c) Viv and its kinetic (pseudo-second-order fitting) of (b) GR and (d) Viv. $[Ca^{2+}]$=15 ppm; $[HCO_3^-]$=80 ppm

(b) and (d)) and the good agreements were obtained ($R^2 > 0.923 – 0.999$). The kinetic constants of GR were similar as $1.84 – 3.01 \times 10^{-2}$ g·(mg·min)$^{-1}$ in the absence and presence of Ca^{2+}/HCO_3^-. However, Viv showed roughly 10 times lower rate (Ca^{2+}: 0.49×10^{-3} g·(mg·min)$^{-1}$; HCO_3^-: 0.30×10^{-3} g·(mg·min)$^{-1}$) compared to the value (3.91×10^{-3} g·(mg·min)$^{-1}$) at ion-free conditions. The calculated adsorption capacities were $53.3 – 53.9$ mg·g^{-1} for GR and $32.3 – 33.0$ mg·g^{-1} for Viv.

The formation of aqueous U(VI) species can be influenced by the groundwater composition, therefore, the U(VI) species distribution in the presence of the ions was calculated as shown in Figure 7. Calcium ion did not affect the U(VI) species distribution while uranyl tricarbonate ($UO_2(CO_3)_3^{4-}$) was newly formed by adding bicarbonate ion ($[HCO_3^-]$=80 ppm). At pH 7, GR surface was positively charged and it would facilitate adsorbing UO_2HPO_4 and $UO_2(PO_4)^-/UO_2(CO_3)_3^{4-}$. The corresponding experimental results were also observed in which rapid and complete adsorption of U(VI) by GR (Figure 4(a)). Viv showed the 13 times lower rate in the presence of HCO_3^- that might be attributed to the electrostatic repulsive force between Viv
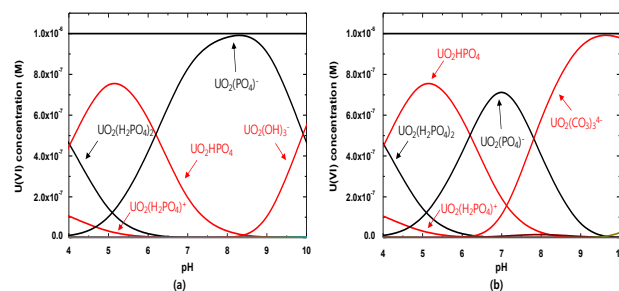

Fig. 7 Chemical distribution of aqueous U(VI) species in the phosphate buffer solution containing (a) $[Ca^{2+}]$ = 15 ppm and (b) $[HCO_3^-]$ = 80 ppm

surface and $UO_2(CO_3)_3^{4-}$. Addition of HCO_3^- have resulted in the formation of $UO_2(CO_3)_3^{4-}$ that was not feasible binding on the negatively charged Viv surface. In addition, carbonate showed the inhibiting effect on the U(VI) adsorption by ferrihydrite at pH > 6 (Waze *et al.* 2003). Interestingly, Ca^{2+} have resulted in 8 times lower adsorption rate of Viv (Figure 6(c)) compared to the value at Ca^{2+}-free condition. The thermodynamic equilibrium calculation showed that Ca^{2+} did not alter the species distribution
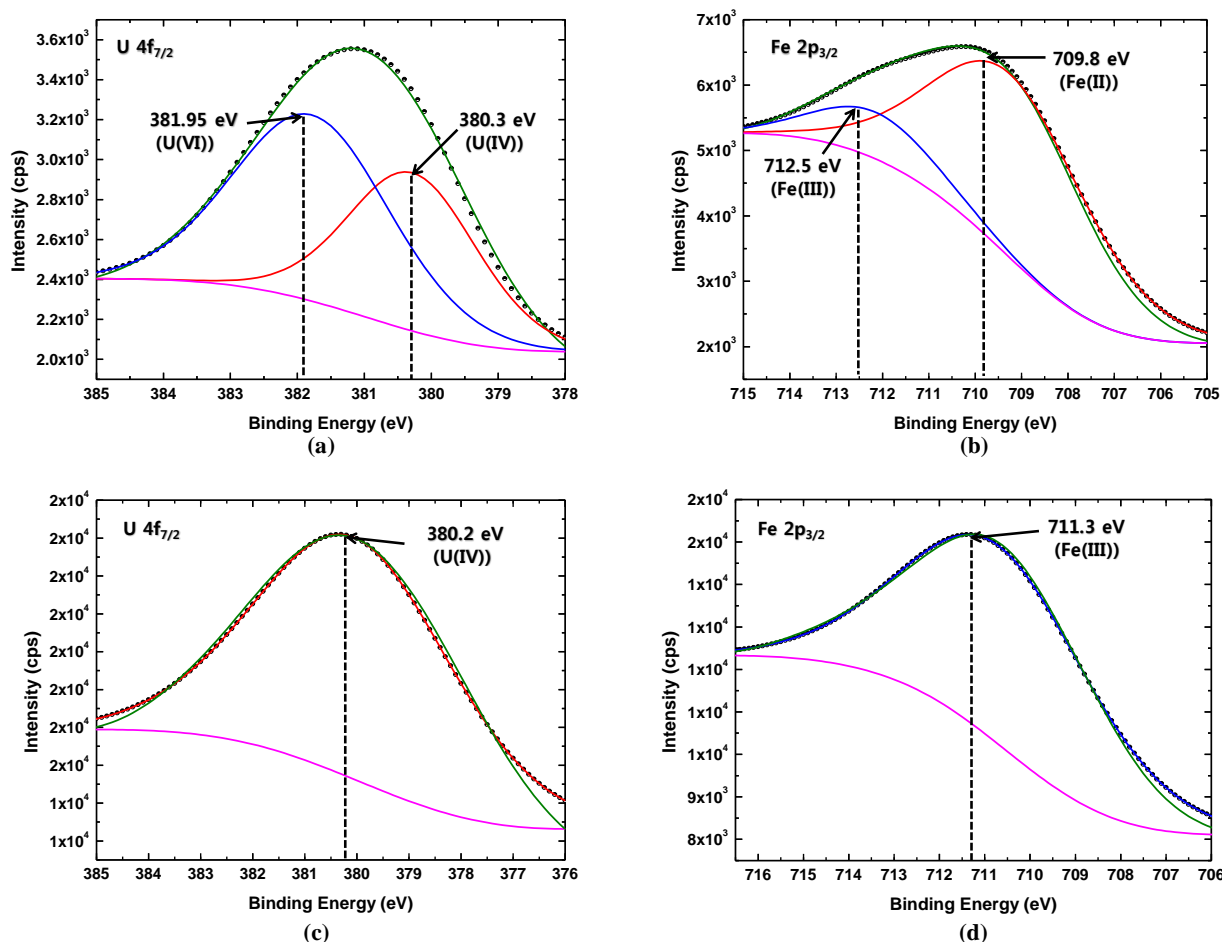
Fig. 8 XPS spectra of U $4f_{7/2}$ and Fe $2p_{3/2}$ from GR surface reacted with U(VI)-phosphates (a) U and (b) Fe spectra after 1h reaction; (c) U and (d) Fe spectra after 7d reaction

(Figure 7(a)), therefore, the lower rate of Viv might have occurred due to competitive adsorption process. Previous studies have reported that the Ca^{2+} binding on the phosphate mineral surface at groundwater condition (Aoba *et al.* 1992). It implies that the competitive Ca^{2+} adsorption on the Viv surface would inhibit the interaction of U(VI) with the adsorptive sites.

3.3 XPS analysis on the reacted minerals

The oxidation states of U and Fe on the mineral surface were measured by XPS. Figure 8 showed the U and Fe spectrum on GR surface at phosphate-rich condition. After 1 h reaction, two distinct U peaks (381.95 and 380.3 eV) were observed indicating the adsorbed U(VI) was partially reduced into U(IV). The dominant Fe spectra was Fe(II) at 709.8 eV and small area with Fe(III) peak was measured at 712.5 eV, respectively. From the 7 d reaction samples, the minor peaks were disappeared and intense single U(IV) and Fe(III) peak were detected at 380.2 and 711.3 eV (Figure 8 (c) and (d)). The results suggest that the aqueous uranyl-phosphates were chemically adsorbed on GR surface in 1 h and it was fully reduced into U(IV) after 7 d reaction.

In addition, the complete oxidation of surface Fe(II) of GR was simultaneously occurred. Figure 9 demonstrates the redox state of U and Fe on the reacted Viv surface. From the 1 h reaction sample, the major U peak was U(VI) (382.4 eV) and the peak with smaller area was U(IV) (380.1 eV). The Fe spectra showed two peaks representing Fe(II) (710.15 eV) and Fe(III) (713.5 eV), respectively. After 7 d reaction, the dominant U peak was shifted to U(IV) at 380.1 eV, but small area of U(VI) was still observed (382 eV) (Figure 7 (c)). The major peak of Fe was Fe(III) phases (712.5 eV) and the small area of Fe(II) (709.5 eV) was remained as shown in Figure 9 (d). The results indicate that the limited reduction of U(VI) was occurred and the Fe(II) phases was partially oxidized into Fe(III) on Viv surface. Concurrent U(VI) reduction-Fe(II) oxidation on the mineral surfaces were confirmed by XPS analysis. The process might have occurred by donating electrons from surface Fe(II) phases to the adsorbed U(VI) species. The U(VI) reducing ability of GR was higher than that of Viv at phosphate-rich conditions and it implies that Fe(II) phases of GR surface has higher redox-activity compared to the that of Viv.
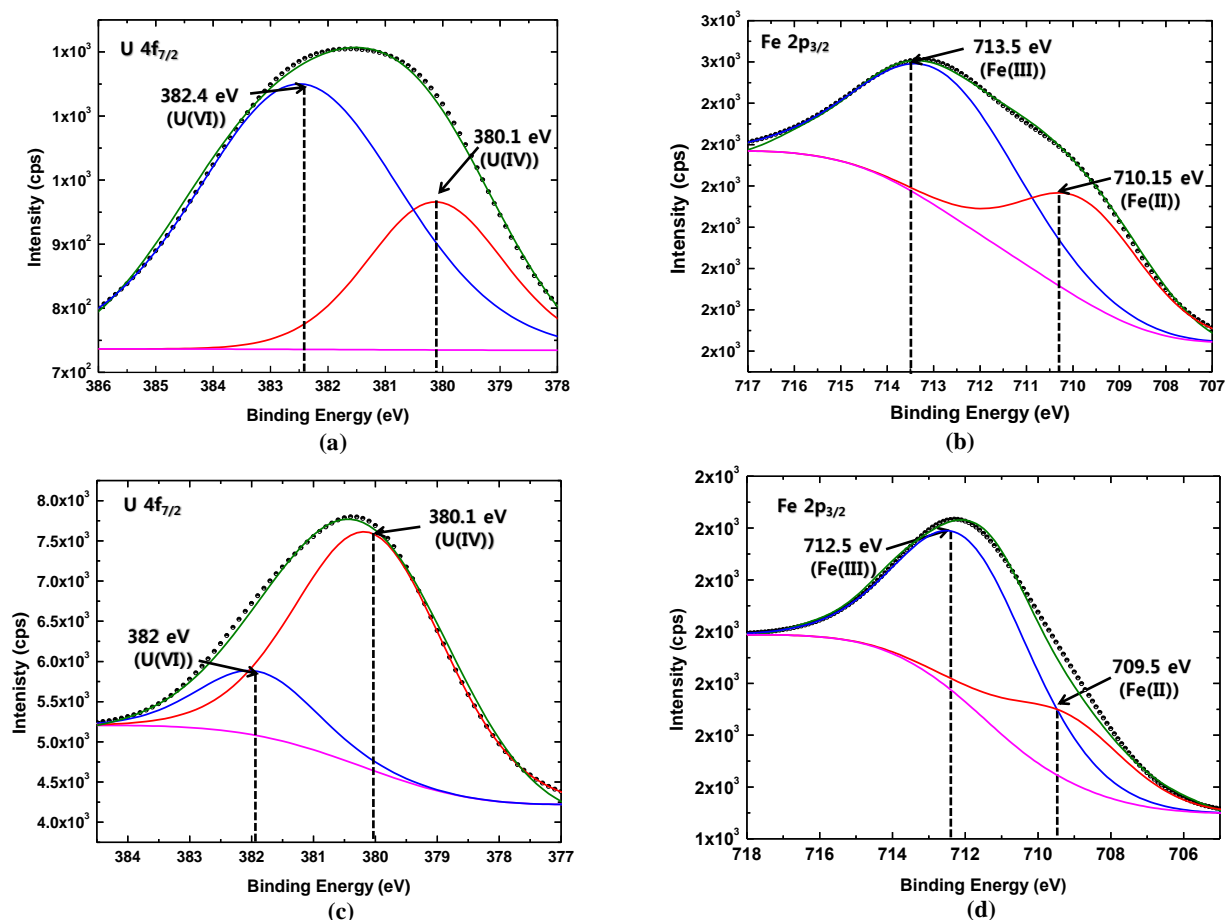
Fig. 9 XPS spectra of U $4f_{7/2}$ and Fe $2p_{3/2}$ from Viv surface reacted with U(VI)-phosphates (a) U and (b) Fe spectra after 1h reaction; (c) U and (d) Fe spectra after 7d reaction

5. Conclusion

We have investigated the aqueous U(VI) removal behavior of GR and Viv at phosphate-rich conditions. The dominant U(VI) species were uranyl phosphate complexes and those were quickly removed by the minerals. The experimental data were well fitted by pseudo-second order kinetic model representing U(VI) was chemically adsorbed on the mineral surfaces. The adsorption kinetic and capacity of GR were faster and higher than that of Viv. It might be attributed to the favorable charge property of GR surface toward neutral/negatively charged U(VI) species. In the presence of Ca^{2+} and CO_3^{2-}, the adsorption performance of GR was not influenced by the ions. However, the competitive adsorption of Ca^{2+} and newly formed $UO_2(CO_3)_3^{4-}$ species have resulted in the 8 – 13 times lower adsorption kinetic of Viv. The chemical reduction of adsorbed U(VI) into U(IV) was confirmed by XPS analysis. GR could fully reduce adsorbed U(VI) in 7 d, however, limited reduction of U(VI) ($\fallingdotseq 80\%$) was observed on Viv surface. The Fe(II) phases on the mineral surface were oxidized into Fe(III) indicating surface Fe(II) might play an electron donor role in the U(VI) reduction process. GR and Viv are the secondary minerals that typically found at metal-reducing bacteria dominant subsurface. Phosphate is essential for microbial metabolism, therefore, GR and Viv-enriched environments would contain high-levels of phosphate. The findings in this study prove that aqueous U(VI) in phosphates-buffer solution was effectively removed by GR and Viv through surface-mediated adsorption process. The adsorbed U(VI) was chemically reduced into immobile U(IV) by receiving electrons from surface Fe(II) phase. It suggests that GR and Viv can be applied to the in-situ remediation technology to retard and long-term immobilize U(VI) transport in groundwater.

Acknowledgments

References

Aamrani, S.E., Gimenez, J., Rovira, M., Seco, F., Grive, M., Bruno, J., Duro, L. and Pablo, J. (2007), "A spectroscopic study of uranium(VI) interaction with magnetite", *Appl. Surf. Sci.,* **253**, 8794-8797. https://doi.org/10.1016/j.apsusc.2007.04.076.

Alves, J., Carvalho, F.P., Falck, W.E., Madruga, M.J., Machado

Leite, L.R., Read, D., Reis, M., Servant-Perrier, A.C. and Steyskal, S. (2004), "Environmental contamination from uranium production facilities and their remediation", *IAEAL-05-00414.*

Amaral, E.C., Amundsen, I., Barisi, D., Booth, P., Clark, D.E., Ditmars, J., Dlouhy, Z., Drury, N., Gehrcke, K., Gnugnoli, G., Hagood, M., Jouve, A., McCallum, B., Lagerwaard, A., Loos, M., Martin, L., Phillips, M., Schaller, A., Slavik, O. and Stevenson, K. (1998), "Characterization of radioactively contaminated sites for remediation purposes", *IAEA-TECDOC-1017.*

Aoba, T., Moreno E.C. and Shimoda, S. (1992) "Competitive adsorption of magnesium and calcium ions onto synthetic and biological apatites", *Calcif. Tissue. Int.*, **51**, 143-150. https://doi.org/10.1007/BF00298503.

Bachmaf, S., Planer-Friedrich, B. and Merkel, B.J. (2008), "Effect of sulfate, carbonate, and phosphate on the uranium(VI) sorption behavior onto bentonite", *Radiochim. Acta,* **96**, 359-366. https://doi.org/10.1524/ract.2008.1496.

Bae, S., Sihn, Y., Kyung, D., Yoon, S., Eom, T., Kaplan, U., Kim, H., Schafer, T., Han, S. and Lee, W. (2018) "Molecular identification of Cr(VI) removal mechanism on vivianite surface", *Environ. Sci. Technol.*, **52**, 10647-10656. https://doi.org/10.1021/acs.est.8b01614.

Bae, S. and Lee, W. (2012), "Enhanced reductive degradation of carbon tetrachloride by biogenic vivianite and Fe(II)", *Geochim. Cosmochim. Ac.*, **85**, 170-186. https://doi.org/10.1016/j.gca.2012.02.023.

Bond, D.L. and Fendorf, S. (2003), "Kinetics and structural constraints of chromate reduction by green rust", *Environ. Sci. Technol.*, **37**, 2750-2757. https://doi.org/10.1021/es026341p.

Cheng, T., Barnett, M.O., Roden, E.E. and Zhuang, J. (2007), "Reactive transport of uranium(VI) and phosphate in a goethite-coated sand column: An experimental study" *Chemosphere,* **68**, 1218-1223. https://doi.org/10.1016/j.chemosphere.2007.01.063.

Crane, R.A., Dickinson, M., Popescu, I.C. and Scott, T.B. (2011), "Magnetite and zero-valent iron nanoparticles for the remediation of uranium contaminated environmental water", *Water. Res.,* **45**, 2931-2942. https://doi.org/10.1016/j.watres.2011.03.012.

Das, D., Sureshkumar, M.K., Koley, S., Mithal, N. and Pillai, C.G.S. (2010), "Sorption of uranium on magnetite nanoparticles", *J. Radioanal. Nucl. Chem.,* **285**, 447-454.

Descostes, M., Schlegel, M.L., Eglizaud, N., Descamps, F., Miserque, F. and Simoni, E. (2010), "Uptake of uranium and trace elements in pyrite (FeS₂) suspensions", *Geochim. Cosmochim. Ac.,* **74**, 1551-1562. https://doi.org/10.1016/j.gca.2009.12.004.

Eglizaud, N., Miserque, F., Simoni, E., Schlegel, M. and Descostes, M. (2006) "Uranium(VI) interaction with pyrite (FeS2): Chemical and spectroscopic studies", *Radiochim. Acta*, **94**, 651-656. https://doi.org/10.1524/ract.2006.94.9-11.651.

Gallegos, T.J., Fuller, C.C., Webb, S.M. and Betterton, W. (2013), "Uranium(VI) interaction with mackinawite in the presence and absence of bicarbonate and oxygen", *Environ. Sci. Technol.,* **47**, 7357-7364. https://doi.org/10.1021/es400450z.

Gavrilescu, M., Pavel, L.V. and Cretescu, I. (2009), "Characterization and remediation of soils contaminated with uranium", *J. Hazard. Mater.,* **163**, 475-510. https://doi.org/10.1016/j.jhazmat.2008.07.103.

Ho, Y.S. and McKay, G. (1999) "Pseudo-second order model for sorption processes" *Process Biochem.*, **34**, 451-465. https://doi.org/10.1016/S0032-9592(98)00112-5

Hua, B. and Deng, B. (2008), "Reductive immobilization of uranium(VI) by amorphous iron sulfide" *Environ. Sci. Technol.,* **42**, 8703-8708. https://doi.org/10.1021/es801225z.

Hudson-Edwards, K.A., Houghton, S. and Taylor, K.G. (2008), "Efficiencies of As uptake from aqueous solution by a natural

vivianite material at 4ºC", *Mineral. Mag.,* **72**(1), 429-431. https://doi.org/10.1180/minmag.2008.072.1.429.

Hyun, S. P., Davis, J.A., Sun, K. and Hayes, K.F. (2012), "Uranium(VI) reduction by iron(II) monosulfide mackinawite", *Environ. Sci. Technol.,* **46**, 3369-3376. https://doi.org/10.1021/es203786p.

Jonsson, J. and Sherman, D.M. (2008), "Sorption of As(III) and As(V) to siderite, green rust (fougerite) and magnetite: Implications for arsenic release in anoxic groundwaters" *Chem. Geol.*, **255**, 173-181. https://doi.org/10.1016/j.chemgeo.2008.06.036.

Livens, F.R., Jones, M.J., Hynes A.J., Charnock, J.M., Mosselmans, J.F.W., Hennig, C., Steele, H., Collison, D., Vaughan, D.J., Pattrick, R.A.D., Reed, W.A. and Moyes, L.N. (2004), "X-ray absorption spectroscopy studies of reactions of technetium, uranium and neptunium with mackinawite", *J. Environ. Radioactiv.,* **74**, 211-219. https://doi.org/10.1016/j.jenvrad.2004.01.012.

Missana, T., Garcia-Gutierrez, M. and Fernndez, V. (2003), "Uranium(VI) sorption on colloidal magnetite under anoxic environment: Experimental study and surface complexation modelling", *Geochim. Cosmochim. Ac.,* **67**(14), 2543-2550. https://doi.org/10.1016/S0016-7037(02)01350-9.

O'Loughlin, E.J., Kelly, S.D., Cook, R.E., Csencsits, R. and Kemner, K.M. (2003), "Reduction of uranium(VI) by mixed iron(II)/iron(III) hydroxide (Green rust): Formation of UO₂ nanoparticles", *Environ. Sci. Technol.,* **37**, 721-727. https://doi.org/10.1021/es0208409.

O'Loughlin, E.J., Kelly, S.D. and Kemner, K.M. (2010), "XAFS investigation of the interactions of U^{VI} with secondary mineralization products from the bioreduction of Fe^{III} oxides" *Environ. Sci. Technol.,* **44**, 1656-1661. https://doi.org/10.1021/es9027953.

O'Loughlin, E.J., Kelly, S.D., Kemner, K.M., Csencsits, R. and Cook, R.E. (2003) "Reduction of Ag^{I}, Au^{III}, Cu^{II}, and Hg^{II} by Fe^{II}/Fe^{III} hydroxysulfate green rust" *Chemosphere*, **53**, 437-446. https://doi.org/10.1016/S0045-6535(03)00545-9.

Payne, T.E., Davis, J.A. and Waite, T.D. (1996), "Uranium adsorption on ferrihydrite-effects of phosphate and humic acid" *Radiochim. Acta,* **74**, 239-243. https://doi.org/10.1524/ract.1996.74.special-issue.239.

Peterson, R.E., Rockhold, M.L., Serne, R.J., Thorne, P.D. and Williams, M.D. (2008), "Uranium contamination in the subsurface beneath the 300 area, Hanford site, Washington", Pacific Northwest National Lab, PNNL-17034; Richland, WA, U.S.A.

Romero-Gonzalez, M.R., Cheng, T., Barnett, M.O. and Roden, E.E. (2007), "Surface complexation modeling of the effects of phosphate on uranium(VI) adsorption", *Radiochim. Acta,* **95**, 251-259. https://doi.org/10.1524/ract.2007.95.5.251.

Schellenger, A.E.P. and Larese-Casanova, P. (2013), "Oxygen isotope indicators of selenite reaction with Fe(II) and Fe(III) hydroxides", *Environ. Sci. Technol.,* **47**, 6254-6262 https://doi.org/10.1021/es4000033.

Scott, T.B., Tort, O.R. and Allen, G.C. (2007), "Aqueous uptake of uranium onto pyrite surfaces; reactivity of fresh versus weathered material", *Geochim. Cosmochim. Ac.,* **71**, 5044-5053. https://doi.org/10.1016/j.gca.2007.08.017.

Selvakumar, R., Ramadoss, G., Menon, M.P., Rajendran, K., Thavamani, P., Naidu, R. and Megharaj, M. (2018), "Challenges and complexities in remediation of uranium contaminated soils: A review", *J. Environ. Radioactiv.,* **192**, 592-603. https://doi.org/10.1016/j.jenvrad.2018.02.018.

Sihn Y., Lee, Y. and Yun, J.I. (2016), "Laser spectroscopic characterization and quantification of uranium(VI) under fluorescence quenching by Fe(II)", *J. Radioanal. Nucl. Chem.*, **308**, 413-423. https://doi.org/10.1007/s10967-015-4428-3.

Sihn, Y., Bae, S. and Lee, W. (2013) "Formation of surface mediated iron colloids during U(VI) and nZVI interaction", *Adv. Environ. Res.*, **2**(3), 167-177. http://dx.doi.org/10.12989/aer.2013.2.3.167

Singh, A., Catalano, J.G., Ulrich, K.U. and Giammar, D.E. (2012), "Molecular-scale structure of uranium(VI) immobilized with goethite and phosphate", *Environ. Sci. Technol.,* **46**, 6594-6603. https://doi.org/10.1021/es300494x.

Veeramani, H., Alessi, D.S., Suvorova, E.I., Lezama-Pacheco, J.S., Stubbs, J.E., Sharp, J.O., Dippon, U., Kappler, A., Bargar, J.R. and Bernier-Latmani, R. (2011), "Products of abiotic U(VI) reduction by biogenic magnetite and vivianite", *Geochim. Cosmochim. Ac.,* **75**, 2512-2528. https://doi.org/10.1016/j.gca.2011.02.024.

Wazne, M., Korfiatis, G.P. and Meng, X. (2003) "Carbonate effects on hexavalent uranium adsorption by iron-oxyhydroxide", *Environ. Sci. Technol*., **37**, 3619-3624. https://doi.org/10.1021/es034166m.

CC